Three-dimensional high-resolution crystallographic observation of the entire volume of microstructurally small fatigue cracks in Ni-Co based superalloy

Hideaki Nishikawa[1]*, Yoshiyuki Furuya[1], Toshio Osada[1], Kyoko Kawagishi, Toru Hara[1]

Affiliation
[1]Research Center for Structural Materials (RCSM), National Institute for Materials Science (NIMS), 1-2-1 Sengen, Tsukuba, Japan 305-0047
*Corresponding author's e-mail address: NISHIKAWA.Hideaki@nims.go.jp

Abstract

The crystallographic features of microstructurally small fatigue cracks (MSFCs) in a Ni-Co-based superalloy were analyzed by using a Xe plasma focused ion beam scanning electron microscope (PFIB-SEM) system in conjunction with electron backscatter diffraction (EBSD) analysis. The crystallographic orientation of the three-dimensional (3D) fatigue crack growth path was successfully observed using a large-volume, high-resolution 3D image. The major parts of the crack surface were close to the {111} slip plane. Our results indicated that the Mode II fatigue crack growth mechanism is locally more predominant than the general blunting-resharpening Mode I fatigue crack growth mechanism, not only in the Stage I region but also in the larger part of the Stage II region of MSFC growth process.

Keywords: small fatigue cracks, crystal orientation, 3D observation, PFIB-SEM, Ni-Co-based superalloy

The fatigue fracture process of metallic materials is divided into fatigue crack initiation and fatigue crack growth (FCG). Forsyth termed the crack initiation process the Stage I region and the subsequent growth process the Stage II region [1]. It is thought that fatigue cracks nucleate and grow along persistent slip bands with intrusion-extrusion of the specimen surface, categorized as fatigue crack initiation mechanism in the Stage I region [2]. In contrast, the crack tip blunting and re-sharpening mechanism that generates fatigue striations on fracture surfaces is well established as the FCG mechanism in the Stage II region [3]. The early part of the Stage II region, which is sensitive to the microstructure, is usually called the Stage IIa region. Hence, microstructural features such as crystallographic facets usually appear on the fatigue fracture surface of this region in contrast from fatigue striations of Stage IIb region. The definition of "microstructurally small fatigue cracks (MSFCs)" [4] also has a similar meaning to the Stage IIa region.

Numerous crystallographic features of MSFCs have been investigated before. In the past, crystallographic features were observed using the etch pit technique on fracture surfaces [5]. In the past couple of decades, electron backscatter diffraction (EBSD) analysis has been commonly used to analyze the growth path of MSFCs [6,7]. This research revealed that part of the fracture surface corresponds to a specific slip plane. However, these methods were able to analyze only a very limited area. More recently, three-dimensional (3D) features of MSFCs have been investigated with high-energy X-ray tomographic techniques using a synchrotron [8–12]. These recent efforts have succeeded in visualizing the discontinuous 3D growth behavior and crystallographic features of MSFCs. However, possibly due to limitations on the spatial resolution of this technique, these 3D analyses were mainly applied to relatively large crack sizes and coarse grain microstructures, typically a few hundreds of micrometers in size. Practically, MSFCs, which tend to measure around 100-μm in the common finer grain microstructures are also important, because more than half of total fatigue life usually elapses before the crack length reaches 200 μm [13].

High-resolution observations are needed to accurately characterize MSFCs of the above sizes. To analyze MSFCs in 3D at high resolution, serial block face (SBF)-SEM analysis was applied [10]. However, this method cannot obtain crystallographic information. Serial sectioning using focused ion beam-scanning electron microscopy (FIB-SEM) with EBSD would therefore be the ideal method in this case. This method has widely been applied [14,15] but if a standard Gallium-FIB is applied, the maximum observable size is limited to around a 20-μm cube. In this study, we used a combination of Xe-plasma FIB (PFIB) and EBSD with a complementary metal oxide semiconductor (CMOS) image detector to counteract these disadvantages: the PFIB can process a larger area 40 times faster than Gallium-FIB, and the CMOS-based EBSD detector can measure 10 times faster than a charge-coupled device (CCD). This method makes it possible to obtain 3D microstructural and crystallographic information on a cube larger than 200 μm in volume with high spatial resolution. We therefore aimed to clarify the crystallographic features of practical MSFCs using a PFIB-SEM system.

The material used in this study was TMW-4M3 forged Ni-Co-based superalloy [16–18] developed for turbine discs in aircraft or land-based gas turbine applications. The alloy has a face-centered cubic (FCC) structure strengthened by fine γ′ precipitates [17]. It has a tensile strength of 1615 MPa and a yielding strength of 1165 MPa at room temperature. Fatigue tests were conducted under fully reversed tension-compression axial loading with a servo hydraulic fatigue testing machine at room temperature. Surface fatigue crack length was measured at intervals using the microscope system [19]. The fatigue specimen size was approximately 4.5 mm wide and 3 mm thick with flat observation face, the same as in our previous study [7]. An artificial sharp notch 60-μm in length was introduced on the specimen surface by FIB. Here, it is worth noting that the size of FIB notch is comparable to the internal inclusion size of the alloy

[18]. The damage due to the FIB notch fabrication was not detected by SEM and EBSD.

3D serial sectioning was conducted using the PFIB-SEM system. The targeted volume measured about 200 x 80 x 70 μm in the form of a rectangular parallelepiped. Serial sectioning observation was carried out under the following conditions: 1,000 images were recorded every 100 nm slice and EBSD patterns were taken every 5 slices. For clear microstructure and crack contrast, scanning ion-induced secondary electron (SIM) imaging was chosen. Segmentation of the 3D fatigue crack volume from SIM images was conducted by using several thresholding methods for 2D and 3D image analysis. The crystal orientations of the crack surface were calculated from the local normal vector of the crack face and the Euler angle value, converted from the RGB values of stacked EBSD images, that is, stacked Euler angle RGB images generated from EBSD data. The measurement error of this analysis is caused by stacking and alignment accuracy between SIM and EBSD images. Hence, the image positions were manually adjusted according to microstructure pattern to suppress the misalignment below 2 degree. Local crack surface angle was calculated from the inner product of local normal vector and loading axis.

Figure 1 shows the fatigue crack growth behavior and fracture surface morphology. Fatigue testing for 3D observation was stopped when the crack length reached 150 μm. As shown in Figure 1b, fatigue crack growth rate and stress intensity factor range of this testing condition were close to the linear region, Stage II region in other words, as described by the long-crack Paris law. The fatigue fracture surface of this region shows the numerous microstructural flat areas which are usually called “facets”. Similar microstructural features were predominant where the area up to 0.2 mm deep away from the specimen surface that corresponds to 15 MPa$\sqrt{\text{m}}$ of ΔK. Figure 2 gives an outline of serial-sectioning observations. Figure 2 a) shows the volume of interest, b) is an example of the observed SIM image showing that the crack can be recognized clear enough to extract it. The inserted image is an enlargement of the area one around the crack tip. Figures 2 c) and d) show an obtained EBSD IPF map and derived kernel-averaging misorientation (KAM) map filtered with Kernel size of 5 x 5, respectively. Plastic deformation around the crack can be evaluated using the KAM map. This will be analyzed elsewhere. Figure 2 e) is a reconstructed MSFC morphology that adds an example image and an IPF map from an arbitrary cross section.

Figure 3 shows 3D MSFC morphologies in detail. The traces of grain boundaries described in Figure 3 a) were determined from fatigue crack configuration and stacked EBSD images. Lots of microstructural facets similar to Fig. 1 c) were observed on the 3D crack face. The facet angle tends to change when the crack crosses the grain boundary. There was no inclusion at least on the crack path, because of the low amount of carbide inclusion in the alloy [17]. As shown in the crystallographic orientation of the crack surface of Figure 3b, most of the facets (blue) were close to the {111} slip plane. Some (red) were close to the {100} plane. As shown

in Figure 3c, the warm-colored area of this Figure, which is approximately perpendicular to the loading axis, tends to correspond to the red area in Figure 3b that is close to the {100} plane. On the other hand, the blue area in Figure 3c tends to correspond to the blue area in Figure 3b which is close to the {111} slip plane. Figure 4 shows stereographic projections of crystallographic and geometric features of MSFC surface as evaluated from the entire data set in Figure 3b. The data of this Figure were evaluated for all surface meshes which were adjusted in advance to the same size. This pole figure clearly indicates that large parts of the crack surface were close to the {111} slip plane. In contrast, the local crack face angle were broadly distributed.

The above investigation reveals that the major MSFCs growth path of this study corresponds to the {111} slip plane of FCC system, even in the Stage II FCG region. The common Mode I fatigue crack growth mechanism is the blunting and re-sharpening mechanism with alternate-slip deformation at the crack tip [3]. According to this mechanism, fatigue cracks propagates along the {001} plane with a pair of {111} slips at the crack tip [3,5]. It therefore appears that the crack surface along the {001} plane in Figure 3b is generated by this common Mode I FCG mechanism. However, the common Stage II FCG mechanism was not the primary FCG mechanism in this study. On the other hand, fatigue crack propagation along the slip plane with shear stress is generally known as the Mode II FCG mechanism in the Stage I region [2]. Stage I FCG mechanisms along the slip plane have therefore usually been investigated at fatigue crack initiation grains and a few of their neighboring grains [2,8,14]. Our experimental results indicate that this Mode II FCG mechanism continues for longer than previously thought. In contrast to our results, previously reported small fatigue cracks in FCC material, analyzed using high-energy X-ray techniques, did not clearly propagate along slip planes [9]. This difference is possible because the observed crack size in previous studies was large enough to transit from the microstructure-sensitive Stage IIa region to the insensitive Stage IIb region. The MSFCs growth features explained above are schematically described in Figure 5.

These results might affect fatigue life estimation strategies of this material. For instance, the shear mode FCG model based on dislocation theory [20], which is widely used to estimate the Stage I FCG region [21,22], may also be useful for estimating the fatigue life of the Stage IIa FCG region. Shibanuma et al. have recently developed a fatigue life calculation method that uses the above FCG model [22]. They reported that their proposed method is able to estimate entire fatigue life. This is possibly because a larger part of the Stage II FCG region than previously expected is microscopically propagated according to the shear mode FCG mechanism.

In summary, it appears that the Mode II fatigue crack growth mechanism locally predominates over the blunting-resharpening Mode I fatigue crack growth mechanism, not only in the Stage I region but also in large part of the Stage IIa region of the MSFC growth process.

However, there are a lot of uncertain factors which possibly change the MSFC growth behavior such as loading condition, crack size, material and so on. For example, Ravi et al. demonstrated that inhomogeneous microstructural stress state ahead of the crack tip associated with the modality of crack growth and local crack closure by in-situ high-energy X-ray diffraction analysis [12]. Therefore, continuous investigation is necessary to confirm the applicability of above results.

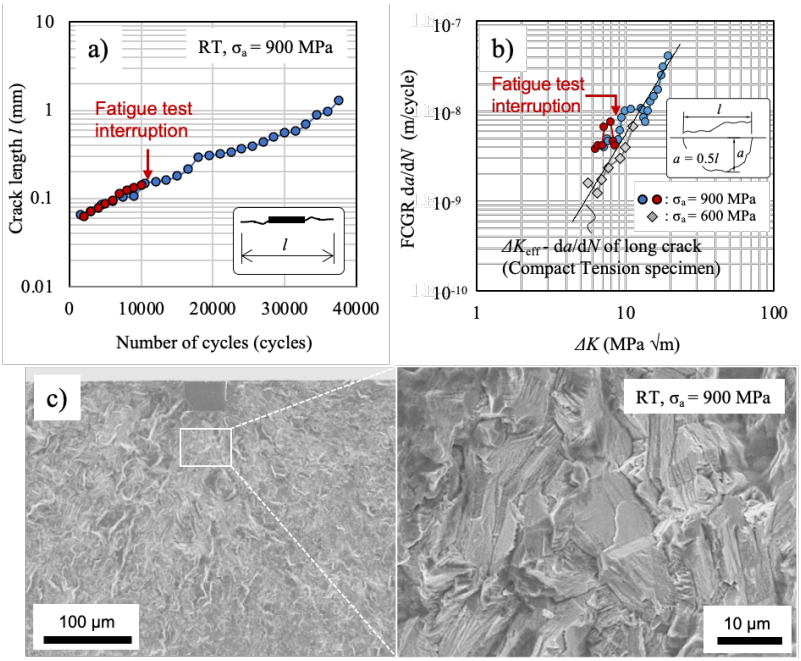

Figure 1 Small fatigue crack growth behavior and fracture surface morphology of broken specimen.

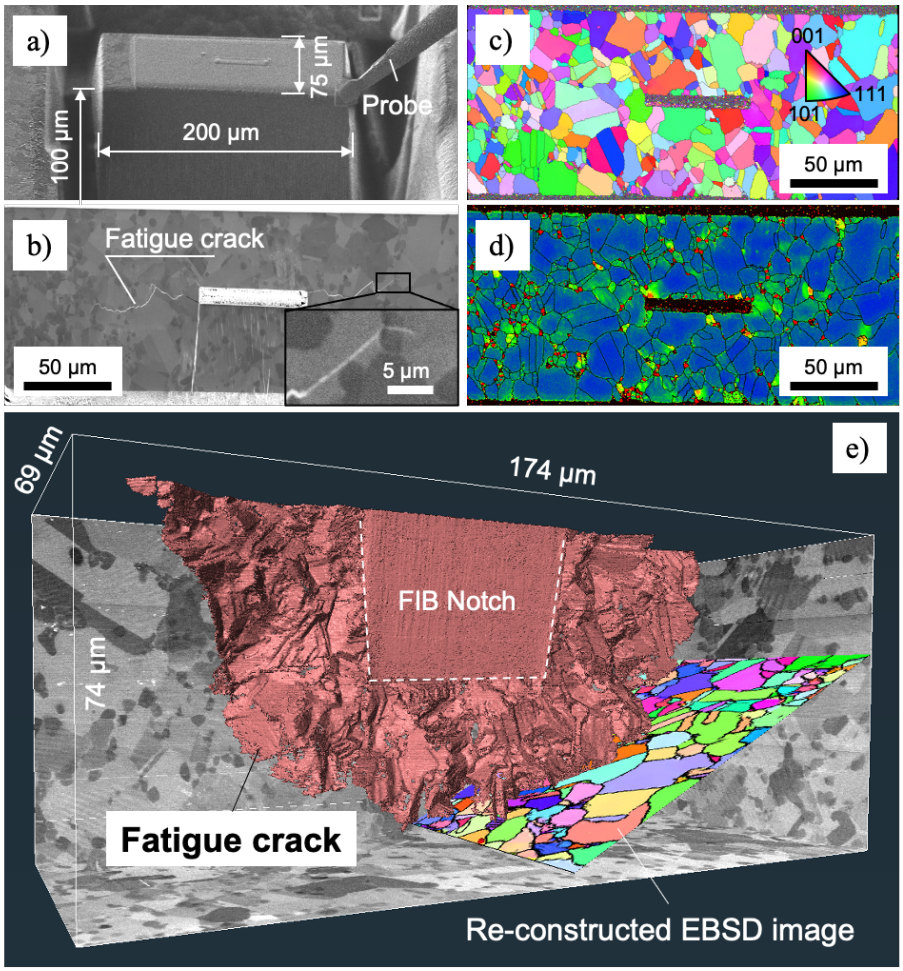

Figure 2 Method of the PFIB-SEM serial-sectioning observation; a) dimension of picked-up sample, b) An example of an observed SIM image, c) IPF map, d) KAM map and e) reconstructed 3D MSFC morphology.

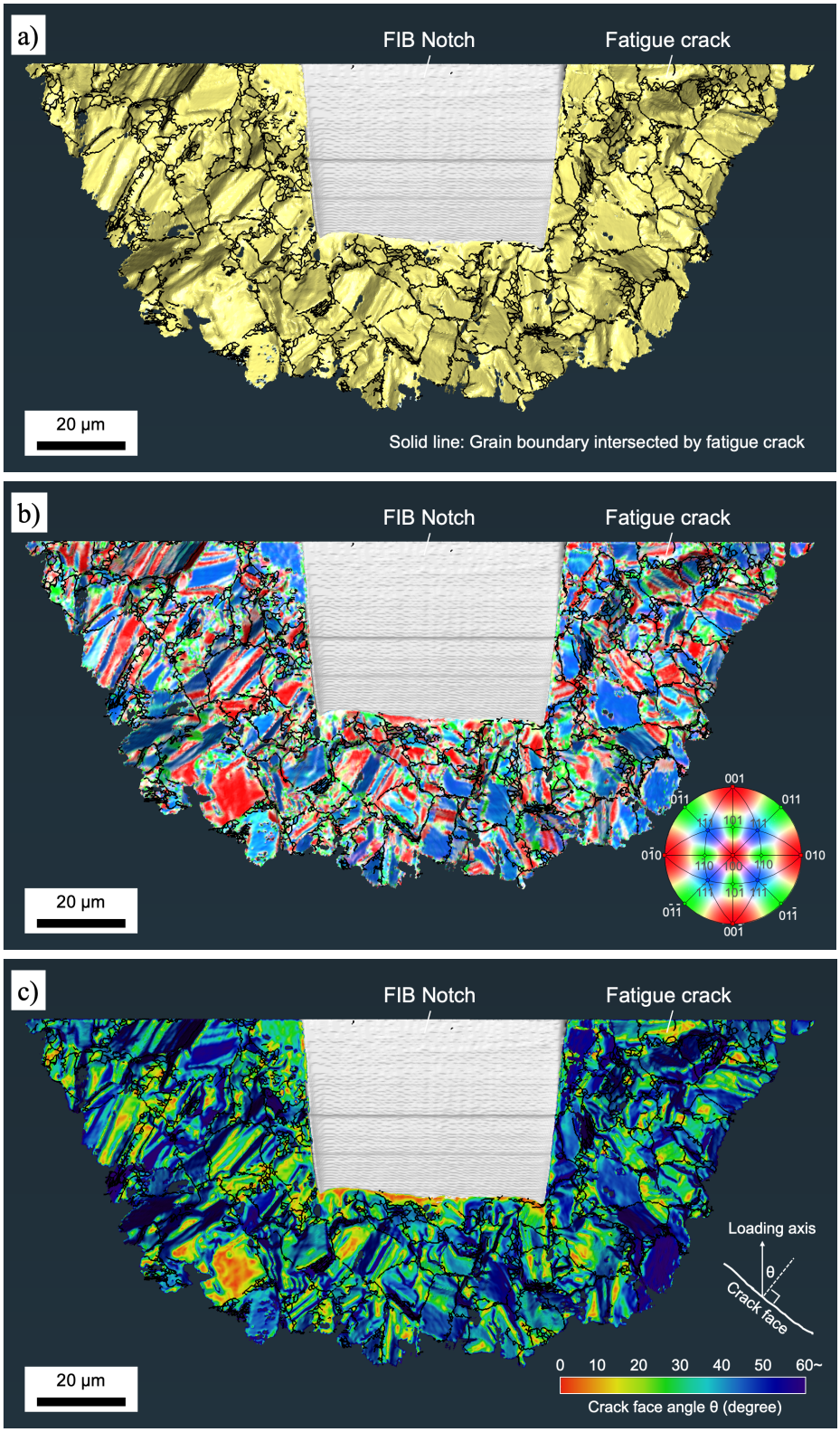

Figure 3 MSFC morphologies represented as a) intersected grain boundaries, b) crystal orientation of the crack surface and c) local crack face angle from the loading axis

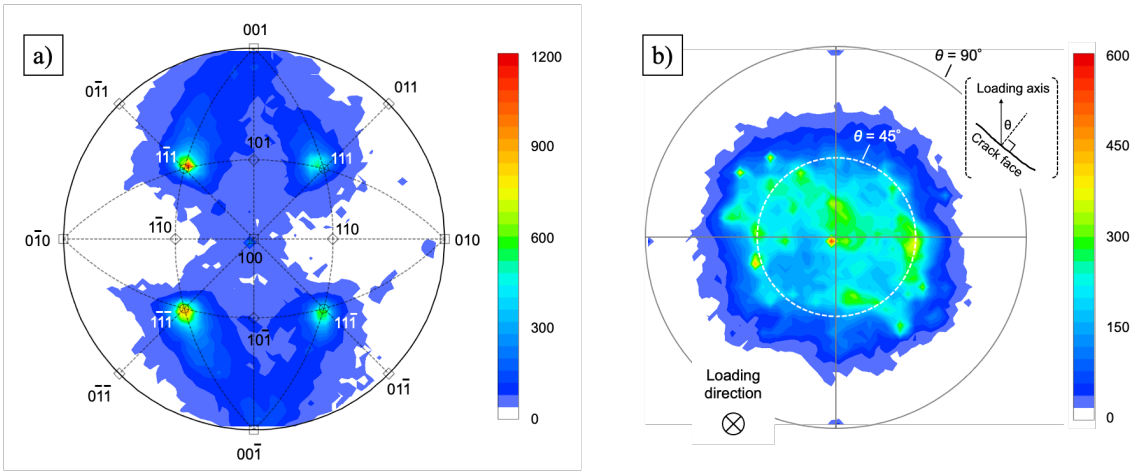

Figure 4 Stereographic projection of a) pole figure and b) local normal vector for entire crack surface

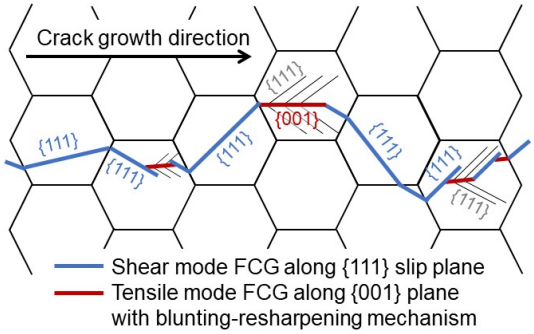

Figure 5 Schematic of MSFC growth path

Acknowledgements

This work was supported by the Council for Science, Technology and Innovation (CSTI), the Cross-ministerial Strategic Innovation Promotion Program (SIP), and “Structural Materials for Innovation” (Funding agency: JST). The PFIB-SEM observation was performed by Ms. Y. Hara at RCSM in NIMS.

References

[1] P.J.E. Forsyth, Fatigue damage and crack growth in aluminium alloys, Acta Metall. 11 (1963) 703–715. doi:10.1016/0001-6160(63)90008-7.

[2] K. Katagiri, A. Omura, K. Koyanagi, J. Awatani, T. Shiraishi, H. Kaneshiro, Early stage crack tip dislocation morphology in fatigued copper, Metall. Trans. A. 8 (1977) 1769–1773. doi:10.1007/BF02646881.

[3] P. Neumann, New experiments concerning the slip processes at propagating fatigue cracks-I, Acta Metall. 22 (1974) 1155–1165. doi:10.1016/0001-6160(74)90071-6.

[4] R.O. Ritchie, J. Lankford, Small fatigue cracks: A statement of the problem and potential solutions, Mater. Sci. Eng. 84 (1986) 11–16. doi:10.1016/0025-5416(86)90217-X.

[5] R. Koterazawa, D. Shimo, Fatigue Crack Propagation and Crystallographic Orientation of an Aluminum Alloy, J. Soc. Mater. Sci. Japan. 25 (1976) 535–541. doi:10.2472/jsms.25.535.

[6] J. Miao, T.M. Pollock, J. Wayne Jones, Crystallographic fatigue crack initiation in nickel-based superalloy René 88DT at elevated temperature, Acta Mater. 57 (2009) 5964–5974. doi:10.1016/j.actamat.2009.08.022.

[7] H. Nishikawa, Y. Furuya, H. Kitano, T. Nakamura, K. Kuwabara, Y. Kanegae, D. Kang, K. Aota, In-situ observation of microstructurally small fatigue crack initiation and growth behaviors of additively-manufactured alloy 718, Mater. Sci. Eng. A. 835 (2022) 142682. doi:10.1016/j.msea.2022.142682.

[8] A. King, W. Ludwig, M. Herbig, J.Y. Buffire, A.A. Khan, N. Stevens, T.J. Marrow, Three-dimensional in situ observations of short fatigue crack growth in magnesium, Acta Mater. 59 (2011) 6761–6771. doi:10.1016/j.actamat.2011.07.034.

[9] A.D. Spear, S.F. Li, J.F. Lind, R.M. Suter, A.R. Ingraffea, Three-dimensional characterization of microstructurally small fatigue-crack evolution using quantitative fractography combined with post-mortem X-ray tomography and high-energy X-ray diffraction microscopy, Acta Mater. 76 (2014) 413–424. doi:10.1016/j.actamat.2014.05.021.

[10] T.J. Marrow, M. Mostafavi, T. Hashimoto, G.E. Thompson, A quantitative three-dimensional in situ study of a short fatigue crack in a magnesium alloy, Int. J. Fatigue.

66 (2014) 183–193. doi:10.1016/j.ijfatigue.2014.04.003.

[11] F. Yoshinaka, T. Nakamura, A. Takeuchi, M. Uesugi, K. Uesugi, Initiation and growth behaviour of small internal fatigue cracks in Ti-6Al-4V via synchrotron radiation microcomputed tomography, Fatigue Fract. Eng. Mater. Struct. 42 (2019) 2093–2105. doi:10.1111/ffe.13085.

[12] P. Ravi, D. Naragani, P. Kenesei, J. Park, M.D. Sangid, Acta Materialia Direct observations and characterization of crack closure during microstructurally small fatigue crack growth via in-situ high-energy X-ray characterization, Acta Mater. 205 (2021) 116564. doi:10.1016/j.actamat.2020.116564.

[13] M. Goto, Statistical Investigation of the Behaviour of Small, Fatigue Fract. Eng. Mater. Struct. 17 (1994) 635–649.

[14] W. Schaef, M. Marx, H. Vehoff, A. Heckl, P. Randelzhofer, A 3-D view on the mechanisms of short fatigue cracks interacting with grain boundaries, Acta Mater. 59 (2011) 1849–1861. doi:10.1016/j.actamat.2010.11.051.

[15] S. Zaefferer, S.I. Wright, D. Raabe, Three-dimensional orientation microscopy in a focused ion beam-scanning electron microscope: A new dimension of microstructure characterization, Metall. Mater. Trans. A Phys. Metall. Mater. Sci. 39 (2008) 374–389. doi:10.1007/s11661-007-9418-9.

[16] C.Y. Cui, Y.F. Gu, H. Harada, D.H. Ping, A. Sato, Phase stability and yield stress of Ni-base superalloys containing high Co and Ti, Metall. Mater. Trans. A Phys. Metall. Mater. Sci. 37 (2006) 3183–3190. doi:10.1007/BF02586152.

[17] T. Osada, Y. Gu, N. Nagashima, Y. Yuan, T. Yokokawa, H. Harada, Optimum microstructure combination for maximizing tensile strength in a polycrystalline superalloy with a two-phase structure, Acta Mater. 61 (2013) 1820–1829. doi:10.1016/j.actamat.2012.12.004.

[18] S. Kobayashi, Y. Ono, T. Osada, S. Ii, K. Kawagishi, Fatigue behavior of a Ni-Co base superalloy for turbine disc applications, Proc. Int. Gas Turbine Congr. (2019) 172-1-172–4.

[19] H. Nishikawa, Y. Furuya, Development of a method for evaluating microstructurally small fatigue crack initiation and growth by using an automatic system for in situ observation in conjunction with a digital-image correlation technique, ISIJ Int. 60 (2020) 2090–2096. doi:10.2355/isijinternational.ISIJINT-2019-823.

[20] K. Tanaka, Y. Akiniwa, Y. Nakai, R.P. Wei, Modelling of small fatigue crack growth interacting with grain boundary, Eng. Fract. Mech. 24 (1986) 803–819. doi:https://doi.org/10.1016/0013-7944(86)90266-3.

[21] F. Briffod, T. Shiraiwa, M. Enoki, Numerical investigation of the influence of rolling texture and microstructure on fatigue crack initiation in BCC polycrystals, Int. J. Fatigue.

107 (2018) 72–82. doi:10.1016/j.ijfatigue.2017.10.019.

[22] H. Ito, Y. Suzuki, H. Nishikawa, M. Kinefuchi, M. Enoki, K. Shibanuma, Multiscale model prediction of ferritic steel fatigue strength based on microstructural information , tensile properties , and loading conditions (no adjustable material constants), Int. J. Mech. Sci. 170 (2020) 105339. doi:10.1016/j.ijmecsci.2019.105339.